JOURNAL OF GUIDANCE, CONTROL, AND DYNAMICS
Vol. 33, No. 4, July–August 2010

Keeping a Spacecraft on a Vertical Circular Collinear Lagrange Point Orbit

Mohammed Ghazy* and Brett Newman†
Old Dominion University, Norfolk, Virginia 23529

DOI: 10.2514/1.47721

A propulsively managed stationkeeping strategy for a spacecraft orbiting a collinear equilibrium point in a three-body system is introduced. A nominal circular solution with nonuniform speed, which is derived from the Jacobi integral equation, employing elliptic integral theory, is used in a plane perpendicular to the line joining the two primaries. Thrust control inputs, which are found to be nonlinear functions of time, are used to negate the instability of the nominal orbit. Analytical relationships for control requirements are developed. Orbit parameters are analyzed and chosen so that the cost of maintaining the nominal orbit is minimized. Resulting thrust requirements are assessed for feasibility with respect to existing propulsion capabilities. Significant freedoms are found to exist for tailoring thrust demands. If proven feasible, the thrust managed orbit could find applications in communications, in situ space measurements, observation platforms, forecasting-warning systems, and loitering. An in situ magnetosphere sampling mission based on a lunar synchronized geopolar orbit is proposed and analyzed using the new results.

Nomenclature

a	=	radius of circular orbit
C	=	Jacobi constant
E	=	complete elliptic integral of the second kind
F	=	incomplete elliptic integral of the first kind
G	=	universal gravitational constant
J	=	Jacobi function
K	=	complete elliptic integral of the first kind
k	=	modulus of the elliptic integral
m_1	=	mass of first primary
m_2	=	mass of second primary, $m_2 \leq m_1$
$\mathbf{r}$	=	position vector of third mass relative to center of mass
$\mathbf{r}_1$	=	position vector of first primary relative to center of mass
$\mathbf{r}_2$	=	position vector of second primary relative to center of mass
r_{12}	=	distance between two primaries
$\boldsymbol{\rho}_1$	=	position vector of third mass relative to first primary
$\boldsymbol{\rho}_2$	=	position vector of third mass relative to second primary
$\boldsymbol{\omega}$	=	angular velocity vector of rotating frame

I. Introduction

IN PREVIOUS research [1], a circular orbit in a plane perpendicular to the line joining the two primaries of a restricted three-body system is used as a nominal generating orbit for an iterative correction process. The nominal orbit is obtained from the Jacobi integral equation and satisfies the motion in the tangential direction in an exact sense and in both normal and binormal directions in bounded and banded senses. Further, the nominal orbit can be made to exactly satisfy the motion in all three axes when control inputs are implemented in the equation of motion such that they negate the instability of this orbit. Both the nominal orbit and control inputs are expressible in explicit analytic form as a function of system parameters and initial conditions.

Though the problem of motion of a spacecraft in the vicinity of one of the libration points of a three-body system has received great attention in the literature, investigations continue based on importance and relevance. Looking for new approximate solutions or even using the already existing ones in different applications is the subject of many research studies up till now. Stationkeeping strategy of a spacecraft in a libration point orbit depends mainly on two parts; the first part is the nominal path the spacecraft follows during one complete period of the motion, and the second part is the control inputs or the thrust forces used to keep the spacecraft close enough to this nominal orbit. The accuracy of the nominal orbit or its closeness to a natural orbit is critical for determining the propulsion requirements in a stationkeeping strategy. For stationkeeping applications, the lack of a benign nominal orbit and an efficient correction process significantly affects the cost in terms of extra thrust demands. Using the linearized equation solution as a nominal path necessarily requires a process of correction that is tedious and lengthy, especially when correction is extended beyond the second term of an expansion technique.

Analogous to the work done in the two-body problem by Tsien [2], motion in the three-body problem with the inclusion of constant thrust acceleration has been investigated [3,4]. In [3] the stability of collinear equilibrium points when applying continuous constant magnitude jet acceleration directed either to one of the primaries (radial thrust) or parallel to the line joining them was investigated. Lyapunov stability analysis gave the sufficient and necessary conditions for gyroscopic stabilization of the two external libration points and indicted that the internal libration point cannot be stabilized. In [4] the stability character and the number of new libration points were investigated under existence of constant radial thrust. Regions of space for existence of libration points were divided according to the magnitude of the thrust acceleration. The case of nonconstant radial low thrust is also included in which the stability character is changed from the case of constant radial thrust.

Farquhar [5] used the solution of the linearized equation of motion about a collinear equilibrium point as a nominal orbit. Corrections to implement nonlinear terms and other perturbing forces, such as solar radiation pressure and gravitational force of a massive body located outside the three-body system and eccentricity in the two primary orbits, are introduced using the linear superposition approach. Thrust control inputs are found to be necessary due to natural instability of the collinear points and stability is attainable through a linear single-axis control with appropriate gains. He also proposed a control of the out-of-plane motion so that a spacecraft at the L_2 libration point is never hidden from the Earth [6]. Heppenheimer [7] proposed a period control to the out-of-plane amplitude and period to ensure synchronization with the in-plane motion and to prevent occultation

Received 19 October 2009; revision received 29 March 2010; accepted for publication 30 March 2010.

*Doctoral Candidate, Department of Aerospace Engineering. Student Member AIAA.

†Professor, Department of Aerospace Engineering. Associate Fellow AIAA.

of a communication link between the L_2 libration point satellite and the Earth. Breakwell et al. [8] used a truncated Fourier series solution to the equation of motion in the vicinity of collinear equilibrium point L_2 as a nominal orbit. Through a quadratic cost criterion involving position variation and control acceleration, three different control strategies, one for three-axis control and two for single-axis control, are used to negate an unstable nominal orbit. Halo and Lissajous trajectories can also be used as nominal orbits in stationkeeping strategies in which correction maneuvers are applied at discrete time intervals [9]. A hovering or humming spacecraft is proposed for stationkeeping purposes at the Lagrange point L_2 in the Earth–moon system [10] with low thrust propulsion needed to prevent attraction by the moon. This technique allows studying the far side of the moon and continuous communication to the Earth. Scheeres and Vinh [11] studied the motion of a spacecraft following an orbit close to another spacecraft moving on an unstable halo orbit. They introduced control laws to stabilize the relative motion in both short term (time is less than one complete period) and long term (one complete period or more) in the sense of Lyapunov, allowing winding of the first spacecraft about the second one in the center manifold of the periodic orbit.

In some particular cases, the nominal orbit is taken to be exactly one of the equilibrium solutions (libration points) and corrections to the nominal solution may not be needed, but control forces are applied to counter any perturbing forces. Lagrange multipliers are used in a typical optimization problem to relate a cost function of the thrust magnitude to the state equations near the libration points. An approximation is required to solve the system of differential equations obtained from applying the necessary conditions of the minimization process, such an approximation is to neglect the Coriolis accelerations [12]. However, the influence of Coriolis terms is found to be substantial [13] when a more exact solution to the same problem is introduced. Following the same method and in a more recent work the nonlinear differential equations of extremals are integrated numerically with the Lagrange multipliers calculated using the linearized equations. Then, more accurate values are obtained by using the shooting technique [14]. For the specific case of obtaining a circular halo orbit, the stationkeeping requirements of control inputs in two different axes are found to be more costly than keeping a spacecraft exactly at the same Lagrange point with single-axis control input [15]. Roithmayr and Kay-Bunnell [16] calculated the velocity increment required from a propulsion system to relocate a spacecraft into the sun–Earth L_2 point, balancing the perturbing gravitational force of the moon, for every lunar period. It is found that if the spacecraft is allowed to move control-free along the line between the sun and the Earth and balancing only the perpendicular motion, the propellant expenditure is reduced to nearly half of that required to control the motion in both directions. A solar sail is used in an attitude control program to achieve a periodic orbit at the L_2 point in the Earth–moon system with an out-of-plane amplitude maximized using certain sail pitch angles [17]. Having no occultation, this orbit is seen from the equatorial region of the Earth and the far side of the moon and can be used in permanent communication between these two regions. However, nonlinear terms in the right-hand side of the variational equations are not considered in the solution. Solar sails are also used to precess the apsidal line of an Earth satellite elliptic orbit to be synchronized with the sun–Earth system rotation for permanent study of the geomagnetic tail [18,19].

In this paper, the solution developed by Ghazy and Newman [1], which is a circular nonuniform speed orbit in a plane perpendicular to the line joining the two primaries, is used as a nominal orbit around a collinear equilibrium point. Thrust forces are applied to keep the spacecraft traversing the nominal orbit, and characteristics and parameters of the nominal orbit are chosen so that motion starts with the minimum initial thrust [20]. In Sec. II, the circular restricted three-body problem, including equations of motion of the third body and the Jacobi integral equation, is reviewed. In Sec. III, the nominal orbit solution is reviewed and characteristics of motion in such an orbit are explained. In Sec. IV, thrust control inputs are included in the differential equation of motion, and thrust components are obtained in a cylindrical coordinate system. In Sec. V, an approach for minimizing initial thrust is discussed. In Sec. VI, analytical relations for thrust supplied velocity increments over one period of motion are obtained in both normal and binormal directions. Parameters for minimum velocity increment are analyzed. Section VII explores the use of these orbits on an in situ Earth magnetosphere sampling mission application. Finally, in Sec. VIII, conclusions are drawn.

II. Circular Restricted Three-Body Problem

The circular restricted three-body problem describes the motion of a negligible mass m_3 in the gravitational field of two other massive bodies: m_1 and m_2, where $m_3 \ll m_2 \leq m_1$. The two massive bodies (primaries) are assumed to move in circular orbits relative to their center of mass not affected by the motion of the negligible mass (third body). Figure 1 shows the circular restricted three-body problem (CRTBP) as expressed in a rotating (synodic) coordinate system in which the x axis is aligned with the line joining the two primaries and pointing to the first primary (m_1). The z axis is the axis of angular momentum of the system. The y axis completes the orthogonal right-handed system. In Fig. 1, cm denotes the center of mass of the system.

The position vector of the third body relative to the center of mass is $\mathbf{r}$. The position vectors of the two primaries relative to the center of mass are $\mathbf{r}_i$ ($i = 1, 2$), and $\boldsymbol{\rho}_1$ and $\boldsymbol{\rho}_2$ are the position vectors of the third body relative to the first and second primary, respectively. These vectors are expressed in the synodic coordinate system as follows:

$$\mathbf{r}_i = x_i \hat{i}, \qquad i = 1, 2 \qquad (x_1 > 0, x_2 < 0) \tag{1a}$$

$$\mathbf{r} = x\hat{i} + y\hat{j} + z\hat{k} \tag{1b}$$

$$\boldsymbol{\rho}_i = (x - x_i)\hat{i} + y\hat{j} + z\hat{k}, \qquad i = 1, 2 \tag{1c}$$

In Eq. (1), $\hat{i}$, $\hat{j}$, and $\hat{k}$ are unit vectors along the coordinates x, y, and z, respectively. Since either primary moves in a circular orbit with constant radius the angular velocity is calculated from the balance between centripetal force, due to motion in a circular orbit, pushing the primary away from the center of the curve and the gravitational force attracting it to the other primary:

$$\omega^2 r_{12} = \frac{G(m_1 + m_2)}{r_{12}^2} \tag{2a}$$

$$\omega^2 = \frac{G(m_1 + m_2)}{r_{12}^3} \tag{2b}$$

$$r_{12} = x_1 - x_2 \tag{2c}$$

Parameter r_{12} is the distance between the two primaries and G is the universal gravitational constant. The angular velocity vector is then expressed as $\boldsymbol{\omega} = \omega\hat{k}$.

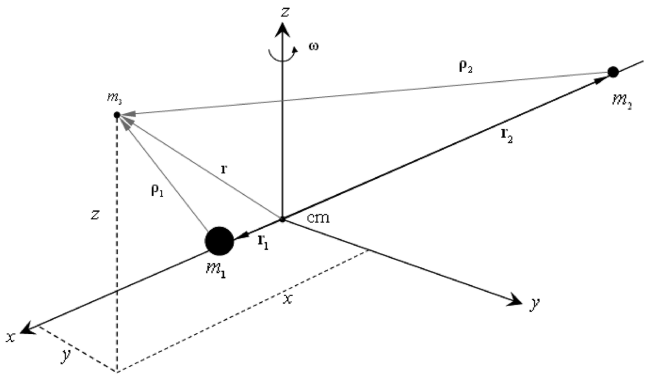

Fig. 1 Circular restricted three-body problem.

The dynamical system representing the motion of the third body has the following Hamiltonian and Lagrangian functions [21]:

$$H = \tfrac{1}{2}(p_1^2 + p_2^2 + p_3^2) + \omega(p_1 q_2 - p_2 q_1) - U \tag{3a}$$

$$L = \tfrac{1}{2}[(\dot{q}_1^2 + \dot{q}_2^2 + \dot{q}_3^2) + 2\omega(q_1\dot{q}_2 - q_2\dot{q}_1) + \omega^2(q_1^2 + q_2^2)] + U \tag{3b}$$

$$U = \frac{Gm_1}{\rho_1} + \frac{Gm_2}{\rho_2} \tag{3c}$$

where the dot on top of a variable denotes differentiation with respect to time; q_i and p_i ($i = 1, 2, 3$) are the generalized coordinates and their conjugate momenta, respectively; U is the forcing function; and ρ_i is the magnitude of $\boldsymbol{\rho}_i$. The generalized coordinates and their associated momenta are defined as follows:

$$q_1 = x, \qquad q_2 = y, \qquad q_3 = z \tag{4a}$$

$$p_1 = \frac{\partial L}{\partial \dot{q}_1}, \qquad p_2 = \frac{\partial L}{\partial \dot{q}_2}, \qquad p_3 = \frac{\partial L}{\partial \dot{q}_3} \tag{4b}$$

From Eqs. (3) and (4) Hamilton's canonical equations are written as follows:

$$\frac{\mathrm{d}q_1}{\mathrm{d}t} = p_1 + \omega q_2, \qquad \frac{\mathrm{d}q_2}{\mathrm{d}t} = p_2 - \omega q_1, \qquad \frac{\mathrm{d}q_3}{\mathrm{d}t} = p_3 \tag{5a}$$

$$\frac{\mathrm{d}p_1}{\mathrm{d}t} = \omega p_2 + \frac{\partial U}{\partial q_1}, \qquad \frac{\mathrm{d}p_2}{\mathrm{d}t} = -\omega p_1 + \frac{\partial U}{\partial q_2}, \qquad \frac{\mathrm{d}p_3}{\mathrm{d}t} = \frac{\partial U}{\partial q_3} \tag{5b}$$

Equations of motion in terms of time derivatives of the coordinates of the third body are obtained through differentiating Eq. (5b) with respect to time and substituting from Eqs. (3–5):

$$\ddot{x} - 2\omega\dot{y} = J_x \tag{6a}$$

$$\ddot{y} + 2\omega\dot{x} = J_y \tag{6b}$$

$$\ddot{z} = J_z \tag{6c}$$

Variable J is the Jacobi function defined as follows:

$$J = \frac{1}{2}\omega^2(x^2 + y^2) + \frac{Gm_1}{\rho_1} + \frac{Gm_2}{\rho_2} \tag{7}$$

The subscripts in the right-hand side of Eq. (6) denote partial derivatives of the Jacobi function with respect to coordinates. These derivatives are

$$J_x = \omega^2 x - \frac{Gm_1}{\rho_1^3}(x - x_1) - \frac{Gm_2}{\rho_2^3}(x - x_2) \tag{8a}$$

$$J_y = \omega^2 y - \frac{Gm_1}{\rho_1^3} y - \frac{Gm_2}{\rho_2^3} y \tag{8b}$$

$$J_z = -\frac{Gm_1}{\rho_1^3} z - \frac{Gm_2}{\rho_2^3} z \tag{8c}$$

The mathematical structure of the equation of motion allows developing a first integral. When multiplying the first, second, and third parts of Eq. (6) by $\dot{x}$, $\dot{y}$, and $\dot{z}$, respectively, then summing the three parts and integrating, one obtains

$$v^2 = 2J - C \tag{9}$$

Equation (9) is known as the Jacobi integral equation, where v is the magnitude of the velocity vector of the third body in the synodic coordinate system and C is the Jacobi constant.

III. Nominal Orbit

For a circular orbit in the CRTBP, in a plane $y'z'$ that is parallel to the yz plane offset by constant distance d_x, the coordinates of the third body are expressed as parametric functions of the orbit radius a and the true anomaly θ as follows:

$$x(t) = d_x \tag{10a}$$

$$y(t) = a\sin\{\theta(t)\} \tag{10b}$$

$$z(t) = a\cos\{\theta(t)\} \tag{10c}$$

where $\theta(t)$ is the angle measured from the z' axis toward the positive end of the y' axis. Together, a and θ determine the location of the third body along the orbit. From the geometry in Fig. 2, or when substituting Eq. (10) into Eq. (1c), the third body in this orbit maintains constant distances from the two primaries:

$$\rho_1 = ((d_x - x_1)^2 + a^2)^{1/2} \tag{11a}$$

$$\rho_2 = ((d_x - x_2)^2 + a^2)^{1/2} \tag{11b}$$

First time derivatives of coordinates are obtained by differentiating Eq. (10) with respect to time. When substituting these derivatives in Eq. (9) the Jacobi integral equation is reformulated into a differential equation of the angle $\theta(t)$:

$$\dot{\theta}^2(t) = \omega^2(\sin^2\{\theta(t)\} - \sin^2\{\theta_0\}) + \dot{\theta}_0^2 \tag{12}$$

where $\theta(t_0) = \theta_0$ and $\dot{\theta}(t_0) = \dot{\theta}_0$ are the initial conditions of the angular displacement and the angular velocity, respectively.

After introducing the transformation $\phi(t) = \pi/2 - \theta(t)$, Eq. (12) with the use of the Legendre normal form of an elliptic integral is integrated over one complete period. A closed form expression of the period of motion T is

$$T = \frac{4k}{\omega}K(k) \tag{13a}$$

where k is the modulus of the elliptic integral and K is the complete elliptic integral of the first kind. The initial conditions are related to the modulus k as follows:

$$k = \left(\cos^2\{\theta_0\} + \left(\frac{\dot{\theta}_0}{\omega}\right)^2\right)^{-1/2} \tag{13b}$$

When Eq. (12) is integrated from an initial time t_0 to a general time t one obtains

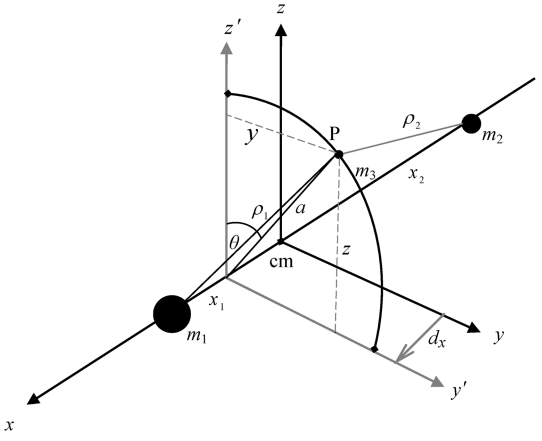

Fig. 2 Third-body nominal circular orbit.

$$\sin\{\theta(t)\} = \mathrm{cn}\left\{-\frac{\omega}{k}(t-t_0) + F\left\{\frac{\pi}{2} - \theta_0, k\right\}, k\right\} \tag{14a}$$

$$\dot{\theta}(t) = \frac{\omega}{k}\mathrm{dn}\left\{-\frac{\omega}{k}(t-t_0) + F\left\{\frac{\pi}{2} - \theta_0, k\right\}, k\right\} \tag{14b}$$

where cn and dn are Jacobi's periodic elliptic functions, and F is the incomplete elliptic integral of the first kind. Detailed derivation of these results appears in [1]. Substituting from Eq. (14) into Eq. (10), coordinates are obtained as functions of time as follows:

$$x = d_x \tag{15a}$$

$$y = a\mathrm{cn}\left\{-\frac{\omega}{k}(t-t_0) + F\left\{\frac{\pi}{2} - \theta_0, k\right\}, k\right\} \tag{15b}$$

$$z = a\mathrm{sn}\left\{-\frac{\omega}{k}(t-t_0) + F\left\{\frac{\pi}{2} - \theta_0, k\right\}, k\right\} \tag{15c}$$

IV. Thrust Control Inputs

The equation of motion is not generally satisfied when substituting the proposed nominal motion from Eq. (10) into Eq. (6). Therefore, to have the third body traverse an exact circular orbit in the $y'z'$ plane, external thrust forces must be applied. Rewriting Eq. (6) including the thrust control inputs in the right-hand side yields

$$\ddot{x} - 2\omega\dot{y} = J_x + u_x \tag{16a}$$

$$\ddot{y} + 2\omega\dot{x} = J_y + u_y \tag{16b}$$

$$\ddot{z} = J_z + u_z \tag{16c}$$

where u_x, u_y, and u_z are the thrust accelerations in the x, y, and z directions, respectively. When substituting the coordinates of the proposed motion from Eq. (10) into Eq. (16), the thrust accelerations are assumed to balance or negate the residue in each direction:

$$u_x = -2\omega a\dot{\theta}\cos\{\theta(t)\} - J_x(d_x, a) \tag{17a}$$

$$u_y = -a\dot{\theta}^2\sin\{\theta(t)\} + a\ddot{\theta}\cos\{\theta(t)\} - J_y(d_x, a, \theta(t)) \tag{17b}$$

$$u_z = -a\dot{\theta}^2\cos\{\theta(t)\} - a\ddot{\theta}\sin\{\theta(t)\} - J_z(d_x, a, \theta(t)) \tag{17c}$$

Before exploring the detail properties of each term in the right-hand side of Eq. (17), reconfiguring Eq. (17) to another coordinate system is considered. In such a system the thrust acceleration components are applied in the binormal, tangential, and normal directions or

$$\begin{bmatrix} u_b \\ u_t \\ u_n \end{bmatrix} = \begin{bmatrix} 1 & 0 & 0 \\ 0 & \cos\theta & -\sin\theta \\ 0 & \sin\theta & \cos\theta \end{bmatrix} \begin{bmatrix} u_x \\ u_y \\ u_z \end{bmatrix} \tag{18a}$$

$$u_b = -a(2\omega\dot{\theta}\cos\{\theta(t)\} + C_x) \tag{18b}$$

$$u_t = 0 \tag{18c}$$

$$u_n = -a(\dot{\theta}^2 + \omega^2\sin^2\{\theta(t)\} + C_z) \tag{18d}$$

where the subscripts b, t, and n in Eq. (18) denote the binormal, tangential, and normal directions, respectively. C_x, C_z are constants defined as follows:

$$C_x = \frac{1}{a}\left(\omega^2 d_x - \frac{Gm_1}{\rho_1^3}(d_x - x_1) - \frac{Gm_2}{\rho_2^3}(d_x - x_2)\right) \tag{19a}$$

$$C_z = -\frac{Gm_1}{\rho_1^3} - \frac{Gm_2}{\rho_2^3} \tag{19b}$$

Equation (19) shows that both C_x and C_z depend on the three-body system under question, the location of the plane motion, i.e., the location of the orbit center on the line joining the two primaries, and the orbit radius. Equation (18) indicates that there is no thrust in the tangential direction required to keep the third body on the nominal orbit, which means that the nominal orbit solution satisfies the equation of motion in the tangential direction. Unfortunately, this is not the case in either the normal or the binormal directions. However, [1] showed that the normal and binormal equations are approximately satisfied in a bounded and banded sense, implying thrust maintenance requirements will not be excessive.

V. Minimum Initial Thrust

Equations (18b) and (18d) indicate the general view to minimize the thrust accelerations. The right-hand side of these two equations consists of two parts: a periodic part with period T and a constant part. Once the three-body system is determined and the location of the orbit center is chosen, the only freedom to minimize the thrust accelerations is the choice of the initial conditions that determine the effect of the periodic part. When the third body starts the motion on the z axis at time $t = t_0$ and an angle $\theta = \theta_0 = 0$, the magnitude u of the total thrust vector at this moment is

$$u_0 = a((2\omega\dot{\theta}_0 + C_x)^2 + (\dot{\theta}_0^2 + C_z)^2)^{1/2} \tag{20}$$

Substituting the initial angular velocity from Eq. (14) with the use of Jacobi elliptic function identities, the initial thrust vector magnitude is rewritten as a function of the modulus of the elliptic integral and the two constants C_x and C_z. These two constants are functions of the radius of the circular orbit and the location of the orbit center, if the three-body system is determined:

$$u_0(k, a, d_x) = a\left(\left(2\omega^2\frac{\sqrt{1-k^2}}{k} + C_x\right)^2 + \left(\omega^2\frac{1-k^2}{k^2} + C_z\right)^2\right)^{1/2} \tag{21}$$

Figures 3–5 show three-dimensional graphs representing the initial thrust vector magnitude as expressed in Eq. (21) for three different

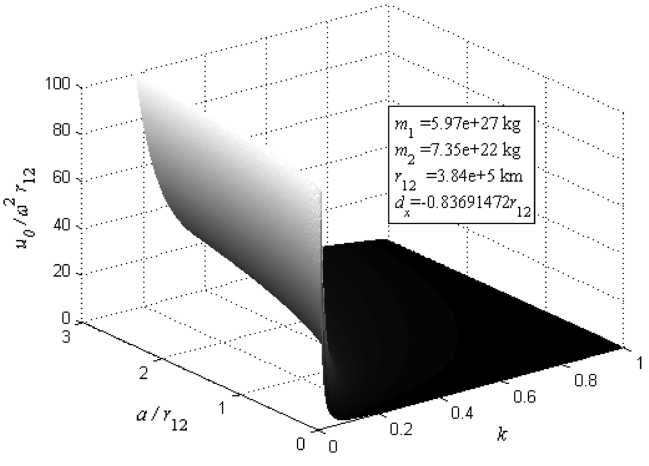

Fig. 3 Initial thrust in L_1 plane of the Earth–moon system.

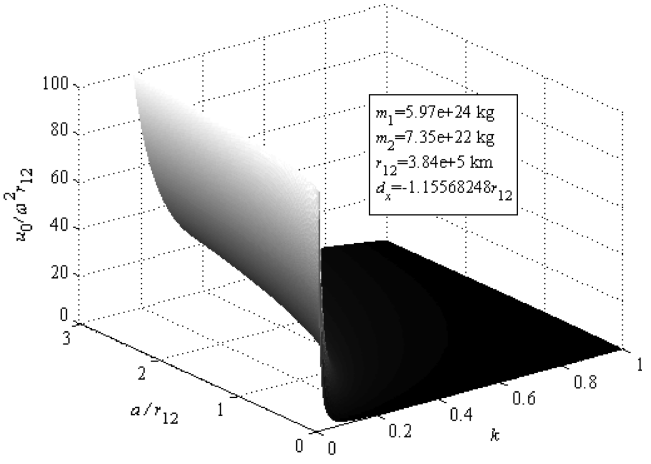

Fig. 4 Initial thrust in L_2 plane of the Earth–moon system.

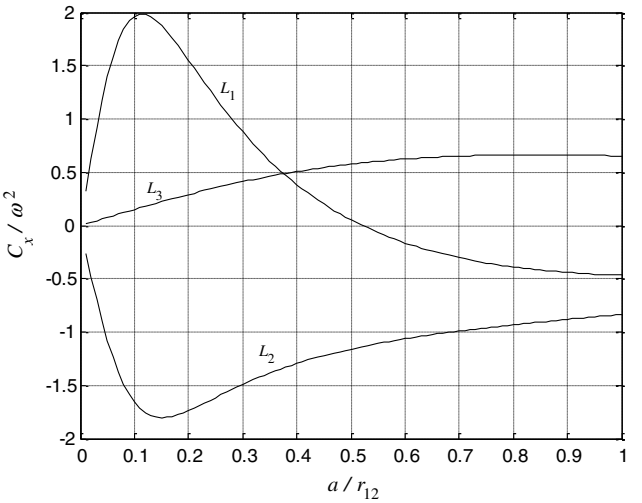

Fig. 6 Constant C_x vs parameters a and d_x.

orbital plane locations corresponding to the collinear equilibrium points of the Earth–moon system:L_1, L_2, L_3. The Earth–moon system is chosen merely as an example.

Surfaces of u_0 at the L_1, L_2, L_3 points appear similar since they are based on the single Eq. (21) and the inherent limiting cases for a, k. However, some differences are noticeable, specifically the curvature of the vertically oriented surfaces as a function of a/r_{12}. Equation (21) indicates that singularity occurs when the elliptic integral modulus approaches its lower limit k: $k \to 0$. In this case, velocity of the third body approaches infinity and the amount of required thrust is unbounded. When the elliptic modulus approaches its upper limit k: $k \to 1$, velocity of the third body approaches zero and the amount of required thrust also approaches its minimum:

$$k \to 0 \Rightarrow \dot{\theta}_0 \to \infty, \qquad u_0 \to \infty \tag{22a}$$

$$k \to 1 \Rightarrow \dot{\theta}_0 \to 0, \qquad u_0 \to a(C_x^2 + C_z^2)^{1/2} \tag{22b}$$

Equation (21) and Figs. 3–5 also indicate that the initial thrust vector magnitude is monotonically increasing with the increase of the orbit radius. This behavior can be explained as the spatial size of the orbit increases, at constant values of initial angular velocity (or elliptic integral modulus magnitude), the effect of gravitational nonlinearity increases and the required initial thrust increases.

The value of u_0 in Eq. (21) depends on two squared quantities and for u_0 to be zero, the two squared quantities should vanish. It is note worthy to investigate values of the two constants C_x and C_z over the domain of orbit radius and location of the orbit center at the three Lagrange collinear points. The locations in the $a - d_x$ space, at which either one or both of the constants C_x and C_z are negative, represent possible minima for the squared quantities in the right-hand side of Eq. (21). In Fig. 6 it is noticed that the sign of C_x varies between positive and negative when the orbit center is located at the Lagrange point L_1, whereas this is not the case at the two other Lagrange points. At point L_3 the value of C_x is always positive, whereas at point L_2 the value of C_x is always negative. Figure 7 shows that the value of C_z is always negative at the three Lagrange points.

Since the elliptic modulus represents a selectable initial condition parameter, a rational process is to choose the elliptic modulus to give minimum initial thrust in one or both directions. When the derivative of the initial thrust vector magnitude with respect to elliptic modulus is set equal to zero, one obtains

$$0 = C_x \frac{k^3}{\sqrt{1-k^2}} + [\omega^2 + C_z]k^2 + \omega^2 \tag{23}$$

since C_x and C_z only depend on a and d_x. Equation (23) may be expanded into a sixth-order polynomial of k. However, for small values of the elliptic modulus ($k \ll 1$), Eq. (23) is simplified to a third-order polynomial of k as follows:

$$0 = C_x k^3 + [\omega^2 + C_z]k^2 + \omega^2 \tag{24}$$

Existence and number of positive real roots for k in Eq. (24) depends on the number of sign changes across all the coefficients, and in

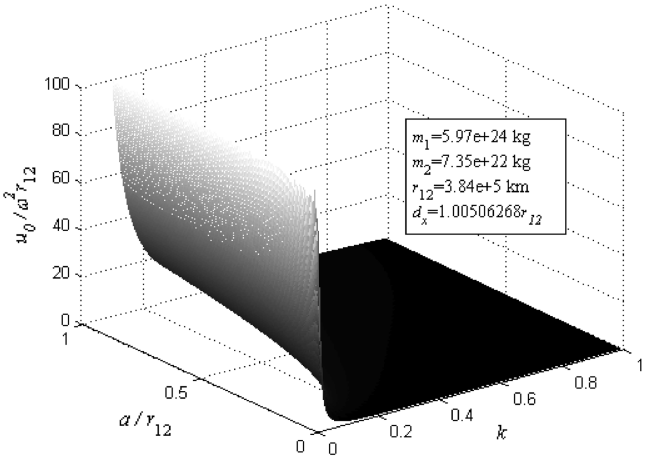

Fig. 5 Initial thrust in L_3 plane of the Earth–moon system.

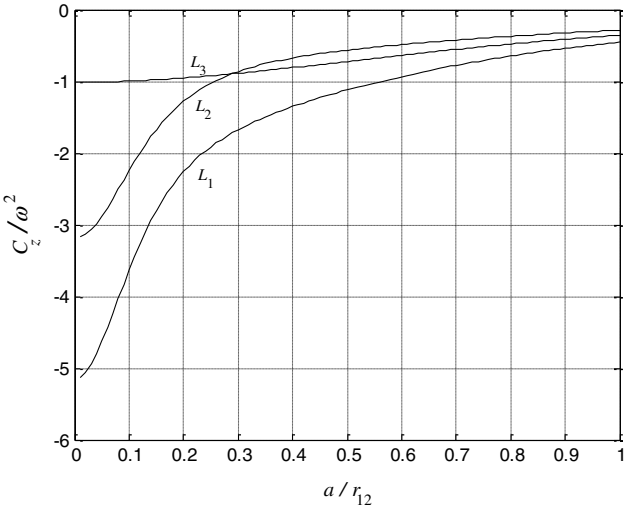

Fig. 7 Constant C_z vs parameters a and d_x.

particular the signs of the first and second term. Three situations for sign change exist:

1) Two sign changes ($C_x/\omega^2 > 0$ and $C_z/\omega^2 < -1$) are possible only at L_1 for the range of orbit radius $a < 0.52106 r_{12}$.

2) One sign change ($C_x/\omega^2 < 0$ and $C_z/\omega^2 > -1$) is possible at L_1 for the range of orbit radius $a > 0.56061 r_{12}$ and at L_2 for the range of orbit radius $a > 0.25650 r_{12}$.

3) One sign change ($C_x/\omega^2 < 0$ and $C_z/\omega^2 < -1$) is possible at L_1 for the range of orbit radius $0.52106 r_{12} < a < 0.56061 r_{12}$ and at L_2 for the range of orbit radius $a < 0.25650 r_{12}$. Figures 6 and 7 indicate that at L_3 constants $C_x/\omega^2 > 0$ and $C_z/\omega^2 > -1$, and thus no sign change occurs in Eq. (24) and no real positive value of the modulus can give a minimum initial thrust.

A few comments on the guidance methodology are given here. The traditional calculus of variations using an adjoint formulation to minimize required thrust is not pursued here, and may not be warranted considering the inherent characteristics of the nominal orbit and its solution framework [1]. In some sense, there is no optimal control problem in this situation since the precise thrust needed to maintain the nominal path is explicitly known and is given by Eqs. (18b) and (18d). This result is different than in the traditional stationkeeping approaches such as target-point strategy and Floquet mode approach, in which the minimization process aims to bring a real orbit to the nominal orbit [22]. Requirements for low thrust here are implemented through choice of orbit parameters and initial conditions, using an analytical framework, as well as for the implementation of thrust in the relevant axes. This approach facilitates a more practical and lower risk orbit maintenance guidance strategy. Equations (18b) and (18d) could be interpreted as a feedback linearization technique (perhaps more correctly labeled feedforward or feedback solvation), which may not be the best control approach under all considerations. The proposed method will continue to be interpreted as a dynamics based analytical approach, similar to the concept of forced Keplerian and non-Keplerian trajectories [23,24].

VI. Velocity Increment

The velocity increment to be supplied by thrusters after one complete period of the third-body motion is analyzed next. The magnitude of the accumulated velocity increment is obtained in the binormal and normal directions when integrating with respect to time equations (18b) and (18d), respectively:

$$\Delta v_b = \int_{t_0}^{T+t_0} |u_b(t)|\,\mathrm{d}t = -\frac{k}{\omega}\int_{\tau_0}^{\tau_f} |u_b\{\tau, k\}|\,\mathrm{d}\tau \tag{25a}$$

$$\Delta v_n = \int_{t_0}^{T+t_0} |u_n(t)|\,\mathrm{d}t = -\frac{k}{\omega}\int_{\tau_0}^{\tau_f} |u_n\{\tau, k\}|\,\mathrm{d}\tau \tag{25b}$$

Variable τ is the argument of the elliptic function [see Eq. (14)] and

$$\tau_0 = F\left(\frac{\pi}{2} - \theta_0, k\right) \tag{26a}$$

$$\tau_f = -\frac{\omega}{k}(T) + F\left(\frac{\pi}{2} - \theta_0, k\right) \tag{26b}$$

Properties of the periodic terms in the integrands of Eq. (25) allow setting the limits of integration as given. Figures 8a–8c show the time history of the periodic terms in the binormal and normal thrust accelerations, respectively. Periods of these thrust acceleration components are $4K$ in Fig. 8a, $2K$ in Fig. 8b, and $2K$ in Fig. 8c. When the initial conditions are chosen such that $t_0 = 0$, $\theta_0 = 0$ one obtains $\tau_0 = K$, $\tau_f = -3K$, and the integration is thus taken from $\tau = K$ to $\tau = 0$ and the results are quadrupled.

Results of integration in Eq. (25) are

$$\Delta v_b(a, d_x; k) = 4a\frac{k}{\omega}KC_x + 8a\omega \tag{27a}$$

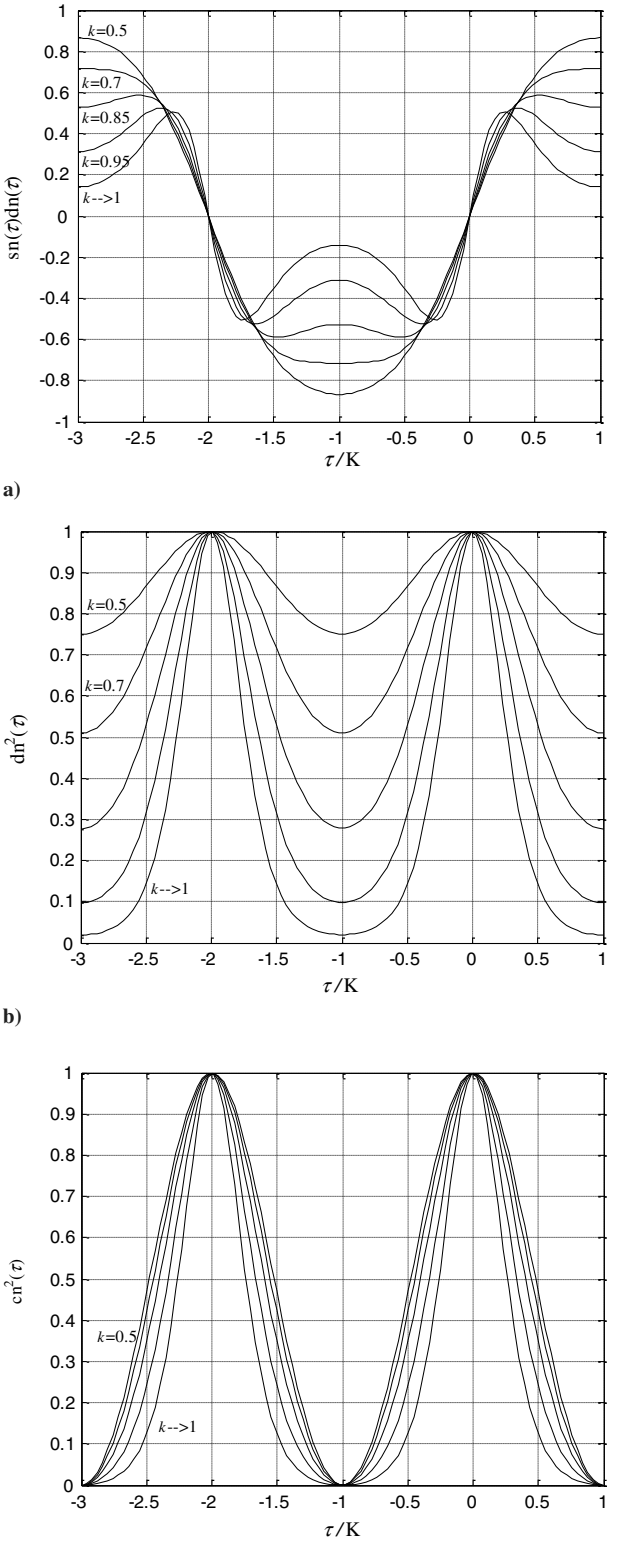

Fig. 8 Plots of time history of periodic functions in a) the binormal thrust acceleration [$\mathbf{sn(\tau)dn(\tau)}$], b) first term in the normal thrust acceleration [$\mathbf{dn^2(\tau)}$], and c) second term in the normal thrust acceleration [$\mathbf{cn^2(\tau)}$].

$$\Delta v_n(a, d_x; k) = 4a\frac{\omega}{k}\left\{2E - \left[1 - k^2 - \left(\frac{k}{\omega}\right)^2 C_z\right]K\right\} \tag{27b}$$

where K and E are the complete elliptic integrals of the first and second kind, respectively. Knowing that $aC_x = J_x$ Eq. (27a) is rewritten as follows:

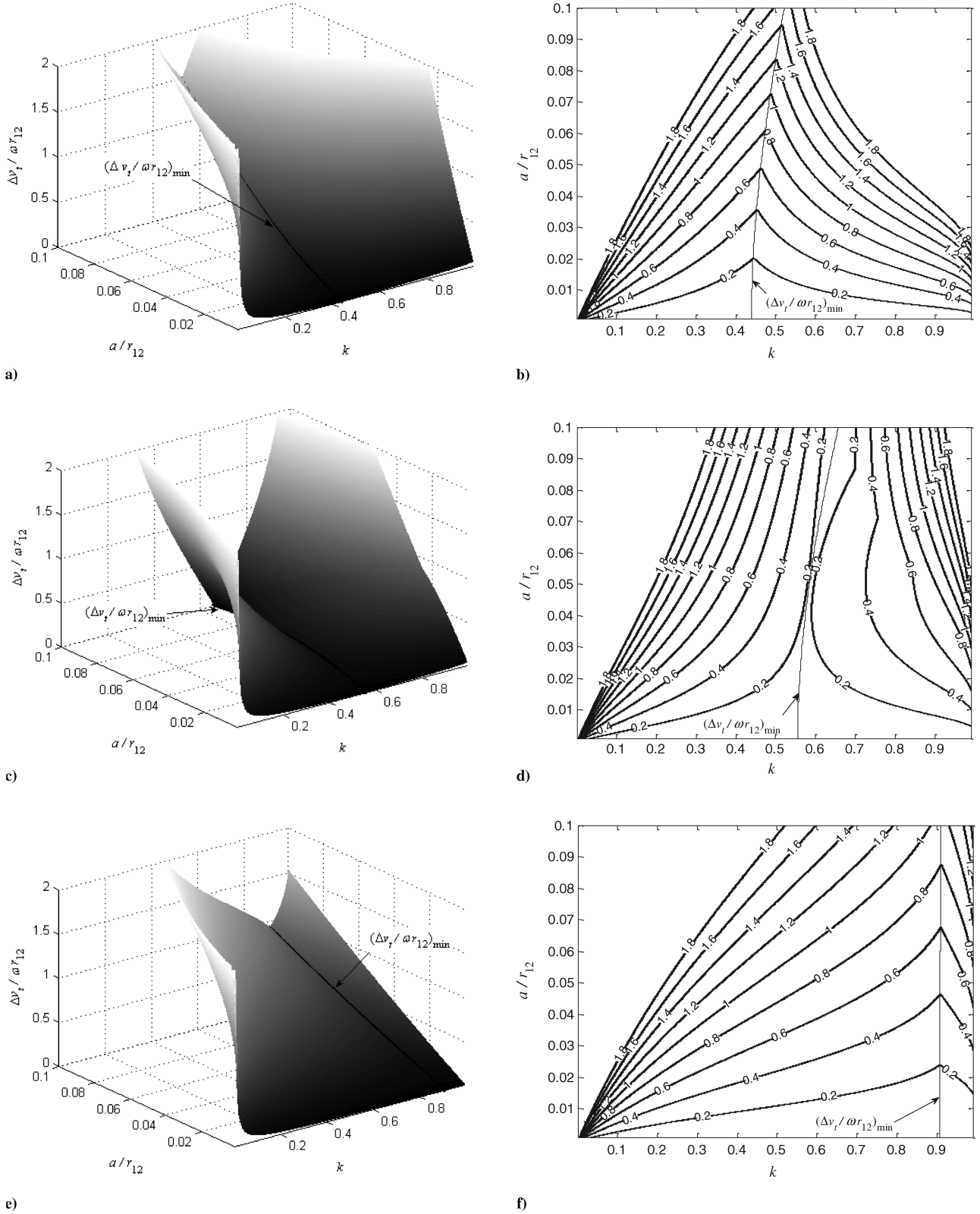

Fig. 9 Plots of total velocity increments and their contour plots at Lagrange point a–b) L_1, c–d) L_2, e–f) L_3.

$$\Delta v_b(a, d_x; k) = 4\frac{k}{\omega} K J_x + 8a\omega \tag{27c}$$

Both velocity increments vanish when the third-body orbit collapses to a zero radius orbit at one of the Lagrange points, i.e., $a = 0 = J_x(d_{L_i})$, $i = 1, 2, 3$. However, if the third body is located at any general point on the x axis, i.e., $a = 0$, $J_x(d_x) \neq 0$, $d_x \neq d_{L_i}$, $i = 1, 2, 3$, there is an increment still needed in the binormal direction and no velocity increment is needed in the normal direction to keep the third body in its location.

Figures 9a–9f show total velocity increments versus orbit radius and modulus of elliptic integral at three different locations of the orbit center on the x axis representing the three Lagrange collinear points for the Earth–moon system. In Figs. 9a–9f Δv_t is the summation of the absolute values of both Δv_b and Δv_n, which are velocity increments in the binormal and normal directions, respectively. Generally, at a certain value of the elliptic modulus the total velocity

increment decreases as the orbit radius decreases. However, this is not the rule for the relation between the total velocity increment and the modulus of elliptic integral. Let the orbit radius and elliptic modulus corresponding to certain minimum total velocity increment along the line $(\Delta v_t/\omega r_{12})_{\min}$ be denoted by a^* and k^*, respectively. At a certain value of the orbit radius $a = a^*$, the total velocity increment increases for any $k \neq k^*$.

To investigate the dimensional values of the velocity increment, at Lagrange point L_1, Fig. 9b shows that the level curve of $\Delta v_t/\omega r_{12} = 0.2$, i.e., $\Delta v_t < 204.96$ m/s is attainable for values of orbit radius $a/r_{12} < 0.02$, i.e., $a < 7680$ km and for all values of elliptic modulus. But for values of orbit radius $a > 7680$ km this level curve is not attainable at any value of the elliptic modulus. In this case, the next indicated minimum level curve in Fig. 9b is that corresponding to$\Delta v_t/\omega r_{12} = 0.4$, i.e., $\Delta v_t < 409.92$ m/ sec applicable for values of elliptic modulus in the range $0.3 < k < 0.6$. Thus for any level curve corresponding to required velocity increment (as in Fig. 9b) and can be attained by certain value of the orbit radius there is a range of values of elliptic modulus from which a value of k can be chosen. As the value of the orbit radius increases the range of values of the elliptic modulus becomes smaller, and at certain value of the orbit radius there is only one value of k that should be chosen and the corresponding velocity increment is a minimum. When the orbit radius exceeds a certain limit this level curve cannot be attained by any value of the elliptic modulus.

A problem of great importance is the determination of initial velocity corresponding to a certain orbit radius. Existence of the modulus in the proposed minimization solution gives an implicit relation between orbit radius and initial velocity. Rewriting Eq. (13b), the initial angular velocity is

$$\dot{\theta}_0 = \frac{\omega}{k}\sqrt{1 - k^2\cos^2\{\theta_0\}} \tag{28}$$

Assuming that the third body starts the motion on the z axis, i.e., $\theta_0 = 0$, the initial angular velocity $\dot{\theta}_0^*$ that gives the minimum total velocity increment is determined from Eq. (28) when values of the elliptic modulus and the orbit radius are chosen to give $(\Delta v_t/\omega r_{12})_{\min}$, as shown in Figs. 9a–9f. Figure 10 shows that the relation between a and $\dot{\theta}_0^*$ is nearly the same when the orbit is located at the L_1, L_2 Lagrange points. At these two points, the value of $\dot{\theta}_0^*$ decreases with a, whereas at the point L_3, the value of $\dot{\theta}_0^*$ is nearly constant with a.

VII. Earth Magnetosphere Sampling Mission

The near-Earth electromagnetic environment and associated dynamic processes remain not well understood. Solar energy inputs, including high-speed electrons, ions, plasma, and electromagnetic disturbances to the magnetosphere, the time-dependent spatial populations of these particles and energy in the Earth radiation belts and magnetic field, and the dissipation and transfer of this energy around the magnetosphere and upper atmosphere are important mechanics that require further study and modeling. Improved knowledge of the Earth electromagnetic physics will allow improved understanding, prediction, and mitigation of detrimental effects, including astronaut radiation risk, spacecraft health deterioration, satellite navigation degradation, radio communication disruption, power grid disturbance, and global warming. Various missions are being considered for this application [25–28]. Use of the new thrust maintained vertically oriented orbits in the Earth–moon system to facilitate in situ tomographic measurements of the magnetosphere, which is considered next. In the current research with the nominal solution maintained by control inputs, three-dimensional structures of the magnetosphere can be sampled by using the fact that the nominal solution is kept in a vertical plane maintaining constant distances from the two primaries all the time, realizing this plane will rotate through the sun–Earth axis and the magnetosphere itself every lunar period. The libration point L_1 is a candidate location for such orbits. Studying natural properties or phenomena that happen in vertical planes at locations d_x other than libration points is also considered. The difference between locations is the cost in terms of thrust fuel demands required to maintain the nominal orbit at that location.

One important application is a vertical orbit at the larger primary, which corresponds to a lunar synchronized geopolar orbit in the Earth–moon restricted three-body problem. Figure 11 depicts this geometry for the hypothetical Earth magnetosphere sampling mission. Magnitudes of thrust supplied velocity increments for this geometry are of interest. When the vertical plane is located at the first primary, i.e., $d_x = x_1$, the constants C_x, C_z take the following forms:

$$C_x = \omega^2\left\{\frac{\mu}{a/r_{12}}\left(1 - \frac{1}{(\rho_2/r_{12})^3}\right)\right\} \tag{29a}$$

$$C_z = \omega^2\left\{-\frac{1}{(\rho_1/r_{12})^3} + \frac{\mu}{(\rho_1/r_{12})^3}\left(1 - \left(\frac{\rho_1}{\rho_2}\right)^3\right)\right\} \tag{29b}$$

where $\mu = m_2/(m_1 + m_2)$ is known as the mass parameter. Substituting $d_x = x_1$ in Eq. (11) and knowing that $x_1 - x_2 = r_{12}$, one obtains

$$\rho_1 = a \tag{30a}$$

$$\rho_2 = (r_{12}^2 + a^2)^{1/2} \tag{30b}$$

When the second primary mass is very small compared to the first primary ($m_2/m_1 = 0.0123$ for the Earth–moon system), the mass parameter approaches its zero lower bound. From Eq. (2b) the angular velocity of the system is rewritten in the case of zero mass parameter as follows:

$$\omega = \sqrt{\frac{Gm_1}{r_{12}^3}} = \sqrt{\frac{Gm_1}{a^3}}\left(\frac{a}{r_{12}}\right)^{3/2} = n\left(\frac{a}{r_{12}}\right)^{3/2} \tag{31}$$

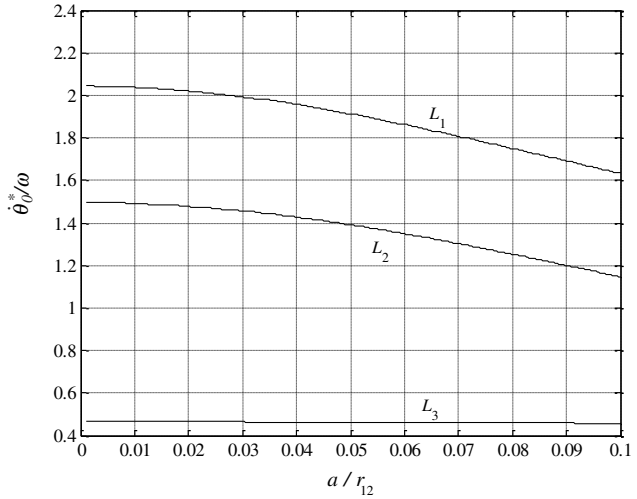

Fig. 10 Initial angular velocity vs orbit radius for minimum total velocity increment.

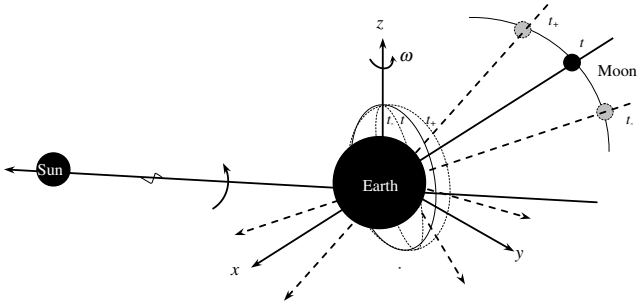

Fig. 11 Geometry of an Earth polar orbit in the Earth–moon and sun–Earth systems.

where n is the mean motion of a satellite in a two-body orbit. In that case, the velocity increments in both binormal and radial directions are

$$\Delta v_b = 8a\omega \tag{32a}$$

$$\Delta v_n = 4a\frac{\omega}{k}\left\{2E(k) - \left[1 - k^2 + k^2\left(\frac{n}{\omega}\right)^2\right]K(k)\right\} \tag{32b}$$

The complete elliptic integrals K and E are functions of the modulus k, which can be substituted from Eq. (13b).

When the initial angular position θ_0 is set to zero, the modulus can be expressed as

$$k = \left(1 + \left(\frac{\dot{\theta}_0}{\omega}\right)^2\right)^{-1/2} \tag{33}$$

Equation (33) indicates that k still depends on the initial angular velocity $\dot{\theta}_0$, which is not yet known. The limiting case (case of zero mass parameter) of a three-body problem is nothing but a two-body problem expressed in a rotating coordinate system centered at the larger primary, since in this case $x_1 \to 0$. Thus, the initial conditions of a two-body circular polar orbit in an inertial frame centered at the larger primary can be used after projection onto the rotating frame of the Earth–moon system to determine the value of $\dot{\theta}_0$. Let a position vector R with inertial frame components be transformed to the rotating frame using the following relation:

$$\mathbf{r} = \mathbf{A}\mathbf{R} \tag{34a}$$

Assuming that the two frames coincide at the initial configuration when $t = t_0 = 0$ the transformation matrix $\mathbf{A}$ is

$$\mathbf{A} = \begin{pmatrix} \cos\omega t & \sin\omega t & 0 \\ -\sin\omega t & \cos\omega t & 0 \\ 0 & 0 & 1 \end{pmatrix} \tag{34b}$$

Differentiating Eq. (34a) with respect to time, the relation between velocity vectors $\mathbf{V}$ and $\mathbf{v}$ in inertial and rotating frames, respectively, are

$$\mathbf{v} = \dot{\mathbf{A}}\mathbf{R} + \mathbf{A}\mathbf{V} \tag{34c}$$

At time $t = 0$ Eq. (34c) can be used to transform the initial velocity from the inertial to rotating frame. Knowing that $R_0 = [0 \quad 0 \quad a]$, $V_0 = [0 \quad an \quad 0]$, and $\mathbf{A}_0 = I_{3\times3}$, then differentiating Eq. (34b) with respect to time and substituting $t = 0$ to obtain $\dot{\mathbf{A}}_0$, one obtains $v_0 = [0 \quad an \quad 0]$. Remembering that the nominal orbit assumes initial velocity vector $v_0 = [0 \quad a\dot{\theta}_0 \quad 0]$, the value of the initial angular velocity is found to be $\dot{\theta}_0 = n$. Substituting this result into Eq. (33) and using Eq. (31) the modulus k takes the following form:

$$k = \left(1 + \left(\frac{n}{\omega}\right)^2\right)^{-1/2} = \left(1 + \left(\frac{r_{12}}{a}\right)^3\right)^{-1/2} \tag{35a}$$

$$k^2\left(\frac{n}{\omega}\right)^2 = 1 - k^2 \tag{35b}$$

Returning to Eq. (32) and substituting for k gives

$$\Delta v_b = 8a\omega \tag{36a}$$

$$\Delta v_n = 8a\omega\left\{\frac{E(k) - K(k)}{k} - kK(k)\right\} \tag{36b}$$

For values of $a \ll r_{12}$ the modulus k is very small and the complete elliptic integrals of the first and second kinds can be expanded using the hypergeometric function $\Im$ [29]:

$$K(k) = \frac{\pi}{2}\Im\left\{\frac{1}{2}, \frac{1}{2}; 1; k^2\right\} = \frac{\pi}{2}\left(1 + \frac{1}{4}k^2 + \frac{9}{64}k^4 + \cdots\right) \tag{37a}$$

$$E(k) = \frac{\pi}{2}\Im\left\{-\frac{1}{2}, \frac{1}{2}; 1; k^2\right\} = \frac{\pi}{2}\left(1 - \frac{1}{4}k^2 - \frac{9}{64}k^4 - \cdots\right) \tag{37b}$$

Finally, substituting from Eq. (37) into Eq. (36), one obtains

$$\Delta v_b = 8a\omega \tag{38a}$$

$$\Delta v_n = (2\pi k)a\omega \tag{38b}$$

Equation (38) shows that if $\omega = 0$ and the rotating frame coincides with the inertial frame the control inputs vanish in both binormal and normal directions. This result means the nominal orbit exists without need for correction in the inertial frame, but the nominal orbit is not naturally maintained in the rotating frame and requires active correction. From Eq. (35a) the modulus k can be approximated to $k = (a/r_{12})^{3/2}$, and noting that the velocity of an Earth satellite on a circular orbit is $V = an$, the velocity increments in Eq. (38) can be normalized using V as follows:

$$\frac{\Delta v_b}{V} = 8\left(\frac{a}{r_{12}}\right)^{3/2} \tag{39a}$$

$$\frac{\Delta v_n}{V} = 2\pi\left(\frac{a}{r_{12}}\right)^3 \tag{39b}$$

Equation (39) shows that the control input in the normal direction is very small compared to that in the binormal direction. The nominal orbit in this case is applied to the Earth–moon system and synchronized with its rotation rate. If a sampling or monitoring mission orbit is designed with an altitude 850 km, then the orbit radius $a = 850 + R_E$, where $R_E = 6357$ km is the Earth's polar radius, and the normalized velocity increments in the binormal and normal directions are 0.0205 and 0.0417×10^{-3}, respectively.

VIII. Conclusions

An exact vertical circular orbit in the three-body problem is achievable using thrust control inputs. Special locations of the orbit plane include but are not limited to the collinear equilibrium points and the two primaries. The control inputs are given as functions of time and are necessary to negate the natural unstability of the nominal solution. Coordinates of a spacecraft moving along the nominal orbit can be predicted at any time and the period of motion can be calculated once the initial conditions are given. The cost for maintaining this orbit in terms of velocity increment per period can be calculated and minimized according to indirect minimization criteria. The nominal orbit can be applied to any three-body system and can be used in different applications.

References

[1] Ghazy, M., and Newman, B., "Analytic Theory for High Inclination Orbits in the Restricted Three Body Problem," *Journal of Guidance, Control, and Dynamics*, Vol. 33, No. 2, March–April 2010, pp. 565–583. doi:10.2514/1.41628

[2] Tsien, H. S., "Take-Off from Satellite Orbit," *ARS Journal*, Vol. 23, No. 4, July–Aug. 1953, pp. 233–236.

[3] Krasilnikov, P. S., and Kunitsyn, A. L., "On the Stabilization of the Collinear Libration Points of the Restricted Circular Three-Body Problem," *Celestial Mechanics and Dynamical Astronomy*, Vol. 15, No. 1, Feb. 1977, pp. 41–51.

[4] Dusek, H. M., "Motion in the Vicinity of Libration Points of a Generalized Restricted Three-Body Model," AIAA/ION Astrodynamics Specialist Conference, AIAA Paper 1965-682, Monterey, CA, Sept. 1965.

[5] Farquhar, R. W., "The Control and Use of Libration Point Satellites," NASA Goddard Space Flight Center, TR-R-346, Washington, D.C., Sept. 1970.

[6] Farquhar, R. W., "Station Keeping in the Vicinity of Collinear Libration Points with an Application to a Lunar Communications Problem," *Space Flight Mechanics, Science and Technology Series*, Vol. 2, American Astronautical Society, New York, 1967, pp. 519–535.

[7] Heppenheimer, T. A., "Optimal Controls for Out-of-Plane Motion about the Translunar Libration Point," *Journal of Spacecraft and Rockets*, Vol. 7, No. 9, Sept. 1970, pp. 1087–1092. doi:10.2514/3.59651

[8] Breakwell, V. J., Kamel, A. A., and Ratner, M. J., "Station-Keeping for a Translunar Communication Station," *Celestial Mechanics*, Vol. 10, No. 3, Sept. 1974, pp. 357–373. doi:10.1007/BF01586864

[9] Howell, K. C., and Pernicka, H. J., "Stationkeeping Method for Libration Point Trajectories," *Journal of Guidance, Control, and Dynamics*, Vol. 16, No. 1, Jan.–Feb. 1993, pp. 151–159. doi:10.2514/3.11440

[10] Vonbun, P. O., "A Hummingbird for the $L2$ Lunar Libration Point," NASA TN-D-4468, April 1968.

[11] Scheeres, D. J., and Vinh, N. X., "Dynamics and Control of Relative Motion in an Unstable Orbit," 2000 AIAA/AAS Astrodynamics Specialist Meeting, Denver, CO, AIAA Paper 2000-4135, Aug. 2000.

[12] Marinescu, A., "Low-Thrust Maneuvers Near the Libration Points," *Journal of Guidance, Control, and Dynamics*, Vol. 2, No. 2, March–April 1979, pp. 119–122. doi:10.2514/3.55846

[13] Marinescu, A., and Dumitrescu, D., "Optimal Low-Thrust Maneuvers Near the Libration Points," *Journal of Guidance, Control, and Dynamics*, Vol. 3, No. 6, March–April 1980, pp. 596–598. doi:10.2514/3.19730

[14] Marinescu, A., and Dumitrescu, D., "The Nonlinear Problem of the Optimal Libration Points Rendezvous in Earth-Moon System," AIAA/AAS Astrodynamics Specialist Conference, AIAA Paper 2000-4433, Denver, CO, Aug. 2000.

[15] Palutan, F., "Stability and Control Problems in Earth-Moon Lagrangian Point $L2$," *Journal of the British Interplanetary Society*, Vol. 47, No. 11, Nov. 1995, pp. 497–504.

[16] Roithmayr, C. M., and Kay-Bunnell, L., "Keeping a Spacecraft on the Sun-Earth Line," 14th AAS/AIAA Space Flight Mechanics Conference, American Astronautical Society Paper 2004-246, Maui, HI, Feb. 2004.

[17] Mcinnes, C. R., "Solar Sail Trajectories at the Lunar $L2$ Lagrange Point," *Journal of Spacecraft and Rockets*, Vol. 30, No. 6, Nov. 1993, pp. 782–784. doi:10.2514/3.26393

[18] McInnes, C. R., and Macdonald, M., "GEOSAIL: Exploring the Geomagnetic Tail Using a Small Solar Sail," *Journal of Spacecraft and Rockets*, Vol. 38, No. 4, July–Aug. 2001, pp. 622–629. doi:10.2514/2.3727

[19] Macdonald, M., Hughes, G. W., McInnes, C., Lyngvi, A., Falkner, P., and Atzei, A., "GeoSail: An Elegant Solar Sail Demonstration Mission," *Journal of Spacecraft and Rockets*, Vol. 44, No. 4, July–Aug. 2007, pp. 784–796. doi:10.2514/1.22867

[20] Ghazy, M., and Newman, B., "Keeping a Spacecraft on a Vertical Circular Orbit Around an Earth-Moon Lagrange Point," AAS/AIAA Astrodynamics Specialist Conference and Exhibit, American Astronautical Society Paper 2009-344, Pittsburgh, PA, Aug. 2009.

[21] Szebehely, V. G., *Theory of Orbits, the Restricted Problem of Three Bodies*, Academic Press, New York, 1967.

[22] Gomez, G., Howell, K., Masdemont, J., and Simo, C., "Station-Keeping Strategy for Translunar Libration Point Orbits," *Advances in the Astronautical Sciences*, Vol. 99, Pt II, 1998, pp. 949–967.

[23] Ross, I. M., Pauls, D. D., and Wilsey, M. S., "Utility of Forced Keplerian Trajectories in Low-Earth-Orbit Maintenance," *Advances in the Astronautical Sciences*, Vol. 87, Pt. I, 1994, pp. 261–273.

[24] Murad, P. A., "Tsien's Method for Generating Non-Keplerian Trajectories," 29th Aerospace Sciences Meeting, Reno, NV, AIAA Paper 91-0678, Jan. 1991.

[25] Mann, I. R., et al., "The Outer Radiation Belt Injection, Transport, Acceleration and Loss Satellite (ORBITALS): A Proposed Canadian Small Satellite Mission for ILWS," *Advances in Space Research*, Vol. 38, No. 8, 2006, pp. 1838–1860. doi:10.1016/j.asr.2005.11.009

[26] Shiokawa, K., Seki, K., Miyoshi, Y., Idea, A., Ono, T., Iizima, M., et al., "ERG–0A Small-Satellite Mission to Investigate the Dynamics of the Inner MagnetoSphere," *Advances in Space Research*, Vol. 38, No. 8, 2006, pp. 1861–1869. doi:10.1016/j.asr.2005.05.089

[27] Sibeck, D. G., and Angelopoulos, V., "THEMIS Science Objectives and Mission Phases," *Space Science Reviews*, Vol. 141, Nos. 1–4, Dec. 2008, pp. 35–59. doi:10.1007/s11214-008-9393-5

[28] Mauk, B. H., Fox, N. J., Sibeck, D. G., and Grebowsky, J. M., "NASA's Radiation Belt Storm Probes (RBSP) Mission," European Planetary Science Congress 2009, Potsdam, Germany, Paper 2009-486, Sept. 2009.

[29] Armitage, J. V., and Eberline, W. F., *Elliptic Functions*, Cambridge Univ. Press, Cambridge, England, U.K., 2006.